Redox Intercalative Polymerization of Aniline in V_2O_5 Xerogel. The Postintercalative Intralamellar Polymer Growth in Polyaniline/Metal Oxide Nanocomposites Is Facilitated by Molecular Oxygen

C.-G. Wu,[†] D. C. DeGroot,[‡] H. O. Marcy,[‡] J. L. Schindler,[‡] C. R. Kannewurf,[‡] Y.-J. Liu,[†] W. Hirpo,[†] and M. G. Kanatzidis*[,†]

Department of Chemistry and the Center for Fundamental Materials Research, Michigan State University, East Lansing, Michigan 48824, and Department of Electrical Engineering and Computer Science, Northwestern University, Evanston, Illinois 60208

Received January 11, 1996. Revised Manuscript Received April 24, 1996[⊗]

Polyaniline can be inserted in $V_2O_5 \cdot nH_2O$ xerogel by in situ oxidative polymerization/intercalation of aniline or anilinium in air. The reaction is facile and topotactic, forming polyaniline as the emeraldine salt. The interlayer separation (5.6 Å) is consistent with a monolayer of polymer chains in the V_2O_5 framework. Evidence is presented that oxygen acts as an electron acceptor both during the in situ reaction and long after intercalation is complete. The crucial role of oxygen in this reaction is probed and discussed. In an alternative route, anilinium is first intercalated and then, in a second step, is oxidatively polymerized in the xerogel upon exposure of the intercalate sample to air. Upon standing in air (aging), two processes occur independently in these materials: (a) the partial reoxidation of the reduced V_2O_5 framework and (b) further oxidative coupling of anilinium and aniline oligomers inside the V_2O_5 layers, leading to longer chain molecules. These observations are supported by several physicochemical data. The magnetic moment of $(PANI)_xV_2O_5 \cdot nH_2O$ decreases gradually upon exposure to air, but it does not change when the sample is stored in vacuum. Gel permeation chromatography (GPC) analysis results show that the molecular weight of polyaniline extracted from aged $(PANI)_xV_2O_5 \cdot nH_2O$ is larger than that extracted from the fresh samples. The thermal stability of polyaniline extracted from aged $(PANI)_xV_2O_5 \cdot nH_2O$ is better than that extracted from fresh samples. All $(PANI)_xV_2O_5 \cdot nH_2O$ samples are paramagnetic with a Curie−Weiss and a temperature-independent van Vleck contribution. Variable-temperature ^2H-wide-line NMR of $(PANI)_xV_2O_5 \cdot nH_2O$ shows that the polymer chains are sterically confined with respect to phenyl ring rotation. The room-temperature conductivity of the freshly prepared $(PANI)_xV_2O_5 \cdot nH_2O$ samples is in the range 10^{-4}−10^{-1} S/cm depending on the degree of polymerization inside the layers, but the conductivity of aged samples is always greater. Room temperature thermoelectric power is negative and varies (−30 to 200 μV/K) depending on the polymer content and the degree of polymerization.

Introduction

During the last several years we have investigated in detail the redox intercalative polymerization of several organic molecules such as aniline, pyrrole, and 2,2′-bithiophene in vanadium oxide xerogel.[1] The corresponding conjugated polymers poly(aniline) (i.e., PANI), poly(pyrrole), and poly(thiophene) form in situ and insert themselves within an electrically conductive mixed-valence V^{4+}/V^{5+} lamellar host. Redox intercalation alters the band structure of vanadium oxide forming bronze-like electrically conductive materials with mixed electronic charge-transport properties.[1] The synthetic methodology we have developed provides a clean and straightforward route to incorporate these intractable polymers in electronically interesting inorganic hosts. The requirement is that the hosts are sufficiently oxidizing and intercalatively accessible. Once in the interior of the host material, the polymer chains search for the lowest attainable energy conformation and orientation. Suitable "lattice matching" between the periodic polymer structure and that of the host tends to maximize the host guest interactions, giving rise to endotaxial order and to a stable nanocomposite system.[2] Endotaxy was observed in the $(PANI)_x$-

[†] Michigan State University.
[‡] Northwestern University.
* To whom correspondence should be addressed. E-mail: kanatzidis@cemvax.cem.msu.edu.
[⊗] Abstract published in *Advance ACS Abstracts,* July 15, 1996.

(1) (a) Kanatzidis, M. G.; Wu, C.-G.; Marcy, H. O.; Kannewurf, C. R. *J. Am. Chem. Soc.* **1989**, *111*, 4139−4141. (b) Wu, C.-G.; Kanatzidis, M. G.; Marcy, H. O.; DeGroot, D. C.; Kannewurf, C. R. *Polym. Mater. Sci. Eng.* **1989**, *61*, 969−973. (c) Wu, C.-G.; Kanatzidis, M. G.; Marcy, H. O.; DeGroot, D. C.; Kannewurf, C. R. NATO Advanced Study Institute, *Lower Dimensional Systems and Molecular Devices*, Metzger, R. M., Ed.; Plenum Press: New York, 1991; pp 427−434. (d) Kanatzidis, M. G.; Wu, C.-G.; Marcy, H. O.; DeGroot, D. C.; Kannewurf, C. R. *Chem. Mater.* **1990**, *2*, 221−224. (e) Wu, C.-G.; Kanatzidis, M. G. *Symposium on Solid State Ionics* Nazri, G., Huggins, R. A., Shriver, D. F., Balkanski, M. Eds.; *MRS Symp. Proc.* **1991**, *210*, 429−442. (f) DeGroot, D. C.; Schindler, J. L; Kannewurf, C. R.; Liu, Y.-J.; Wu, C.-G.; Kanatzidis, M. G. *Symposium on Submicron Multiphase Materials*; Baney, R., Gilliom, L., Schmidt, H., Hirano, S.-I., Eds.; *Mater. Res. Soc. Symp. Proc.* **1992**, 133−138.

S0897-4756(96)00023-3 CCC: $12.00 © 1996 American Chemical Society

FeOCl system where, along the [101] direction, the chloride ion spacings on the surfaces of FeOCl layers are in good registry with the nitrogen atoms of the PANI chains.[2] In this system the strong guest−host interactions occur in the form of NH- - -Cl hydrogen bonding. Since the $V_2O_5 \cdot nH_2O$ xerogel does not display three-dimensional order, the issue of in-plane guest arrangement in its intercalates is much harder to address. Nevertheless, guest−host interactions similar to those found in FeOCl (e.g., NH- - -O═V hydrogen bonding) are expected to occur in the xerogel as well, albeit on a shorter length range given that corresponding good lattice matching may not exist between PANI and the xerogel. We note, however, that lattice matching between the host and the guest is neither necessary nor sufficient to obtain an intercalative nanocomposite. Complicating the problem of determining the guest arrangement is the lack of accurate structural information on the in-plane structure of V_2O_5 xerogel.[3] Another important issue in work of this type is the mechanism of the intercalation/oxidation/polymerization and the correct sequence of these events. Although molecular level mechanisms in heterogeneous systems are very hard to probe, various control experiments could be employed to provide some information at the molecular, mesoscopic, or macroscopic scale.

The formation of PANI from anilinium in vanadium oxide gels is relatively fast. It is presumed that the first step in the insertion of PANI is intercalation of the monomer between the V_2O_5 layers. One way to follow the oxidation of aniline by vanadium oxide would be to trap anilinium ions between the layers of the host and then observe their conversion to polyaniline (PANI) upon oxidative initiation of the polymerization process. The challenge is to prevent the anilinium ions from being oxidized by $V_2O_5 \cdot nH_2O$ before controlled polymerization can be initiated. We accomplished this by satisfying the oxidative power of $V_2O_5.nH_2O$ from a different electron source such as iodide. Oxidation of the material was then induced by allowing prolonged exposure to air. The spectroscopic and physicochemical characterization and charge-transport properties of the lamellar nanocomposite materials $(PANI)_xV_2O_5 \cdot nH_2O$ are described here in detail for the first time.

Experimental Section

Reagents. NaOH, HCl, $NaVO_3$, 2,6-dimethylaniline, $(NH_4)_2S_2O_8$, dimethyl sulfoxide (DMSO), *N*-methylformamide (NMF), 1,4-bis[2-(5-phenyloxazolyl)]benzene (POPOP), *N*,*N*′-bis(*p*-methylbenzylidene)-α,α-bi-*p*-toluidine (BMBT), HPLC grade *N*-methylpyrrolidinone (NMP), and tetrahydrofuran (THF) were purchased from commercial sources and used without further purification. CH_3CN and $C_6H_5NH_2$ were dried with CaH_2 and distilled under vacuum prior to use. Perdeuterated aniline was purchased from Cambridge Isotope Laboratories, Cambridge, MA.

Physicochemical Methods. Elemental analyses were done by Galbraith Laboratories, Knoxville, TN, and Oneida Research Services, Inc., Whitesboro, N.Y. Fourier transform infrared (FTIR) spectra were recorded from pressed KBr pellets using a Nicolet 740 FTIR spectrometer. X-ray powder diffraction studies were carried out with a Phillips XRG-3000 instrument using Ni-filtered Cu Kα radiation or a Rigaku-Denki/RW400F2 (Rotaflex) X-ray powder diffractometer with a rotating anode operating at 45 kV and 100 mA. Transmission-mode diffraction patterns and accurate *d* spacings were obtained with the latter instrument from film or powder samples. Oxygen consumption was followed with a YSI Model 53 oxygen monitor in a closed cell. The oxygen concentration measured with degassed distilled water is defined as 0% and that measured with water saturated with oxygen at room temperature is defined as 100%. Oxygen consumption measurements were made in known time intervals after reaction of the aniline monomer with V_2O_5 xerogel had begun.

Gel permeation chromatography (GPC) for molecular weight measurements was performed with a Perkin-Elmer 250 HPLC with binary LC pump and LC-235 diode array UV/vis detector and with a Shimadzu LC-10A HPLC system. The column used was a PLgel 10 mm mixed B column which has a column efficiency of more than 35 000 plates/m. In a typical procedure, 5 mg of emeraldine base was dissolved in 1.5 mL of NMP. The mixture was then filtered through a 4500 Å pore size filter which was purchased from Phenomenex Inc., Torrance, CA. The column and detector were maintained at room temperature (18 °C). The injection volume was 10 mL, and the flow rate was 0.2 mL/min; a 0.5% LiCl solution in *N*-methyl-2-pyrrolidinone (NMP) was used as an eluent. Monodispersed polystyrene standards (purchased from Polymer Laboratories Inc., Amherst, MA) with molecular weights ranging from 580 to 7 100 000 were used for constructing the calibration curve. Two model compounds, 1,4-bis[2-(5-phenyloxazolyl)]benzene (POPOP) and *N*,*N*′-bis(*p*-methylbenzylidene)-α,α-bi-*p*-toluidine (BMBT) with structures more closely resembling those of aniline oligomers, were used to further correct the molecular weight obtained with the polystyrene calibration.

Thermogravimetric analysis (TGA) and differential scanning calorimetry (DSC) were performed with Shimadzu TGA-50 and DSC-50 thermal analysis systems using dry oxygen or nitrogen as carrier gases. The TGA experiments were run from room temperature to 1000 °C (or 800 °C) at a linear heating rate of 10 °C (or 5 °C) per minute. DSC experiments were run at temperatures between 20 and 500 °C under nitrogen with a heating rate of 5 °C/min.

Electron paramagnetic resonance (EPR) spectra were recorded on a Varian E-4 EPR spectrometer at room temperature or liquid nitrogen temperature. The solid samples were scanned from 2900 to 3900 G at 8−32 G field modulation with 0.1 s time constant. The field was calibrated with 2,2-diphenyl-1-picrylhydrazyl (DPPH, $g = 2.0036$). Variable-temperature magnetic susceptibility data were obtained on a S.H.E. Corp. SQUID system at 5 T applied magnetic field using samples inside polyethylene bags. All data were corrected for diamagnetic contributions. The instrument was calibrated with a sample of $HgCo(SCN)_4$.

Scanning electron microscopy (SEM) studies were done on a JEOL-JSM 35CF microscope operating at 20 kV and equipped with a TRACOR Northern energy-dispersive spectroscopy (EDS) analysis system. The samples for SEM imaging were mounted on Al stubs with graphite paint without further coating. Transmission electron microscopy (TEM) and electron diffraction were done with a JEOL-100 CX(II) operating at 100 kV. Samples for electron diffraction studies were dispersed in acetone, sonicated for 10 min, and then deposited in holey film-coated copper grids. The *d* spacings calculated from the diffraction patterns (Bragg rings) were calibrated with an aluminum standard after each measurement.

Deuterium Wide-Line Nuclear Magnetic Resonance Studies. Perdeuterated aniline (98 atom % deuterium) was

(2) (a) Wu, C.-G.; DeGroot, D. C.; Marcy, H. O.; Schindler, J. L.; Kannewurf, C. R.; Bakas, T.; Papaefthymiou, V.; Hirpo, W.; Yesinowski, J.; Liu, Y.-J.; Kanatzidis, M. G. *J. Am. Chem. Soc.* **1995**, *117*, 9229−9242. (b) Kanatzidis, M. G.; Wu, C.-G.; Marcy, H. O.; DeGroot, D. C.; Schindler, J. L.; Kannewurf, C. R.; Benz, M; LeGoff, E. *Supramolecular Chemistry in Two and Three Dimensions*; Bein, T., Ed.; *ACS Symp. Ser.* **1992**, *499*, 194−219. (c) Kanatzidis, M. G.; Wu, C.-G.; DeGroot, D. C.; Schindler, J. L.; Benz, M; LeGoff, E.; Kannewurf, C. R. NATO Advanced Study Institute in *Chemical Physics of Intercalation;* Bernier, P., Fischer, J. E., Roth, S., Solin, S., Eds.; Plenum Press: New York, 1993; pp 63−72.

(3) (a) Yao T.; Oka,Y.; Yamamoto, N. *Mater. Res. Bull.* **1992**, *27*, 669−675. (b) Yao T.; Oka,Y.; Yamamoto, N. *J. Mater. Chem.* **1992**, *2*, 331−336. (c) Yao T.; Oka,Y.; Yamamoto, N. *J. Mater. Chem.* **1992**, *2*, 337−340 (d) Legendre, J.-J.; Livage, J. *J. Colloid Interface Sci.* **1983**, *94*, 75−83. (e) Livage, J. *Chem. Mater.* **1991**, *3*, 573−593.

purchased from Cambridge Isotope Laboratories. It was converted to the emeraldine salt form by a procedure described in the synthesis section below. Selectively deuterated aniline (N,N-d_2) was prepared by stirring aniline with 98% D_2O for 2 days. The ^2H NMR measurements were carried out on perdeuterated $(PANI)_xV_2O_5{\cdot}nH_2O$ prepared as described above. ^2H NMR spectra were obtained at 9.4 T at a frequency of 61.4 MHz on a Varian VXR-400S solids spectrometer, using a high-power variable-temperature wide-line probe with a 5 mm diameter solenoidal coil that provided 90° pulse lengths of typically 2.8 μs. The following composite-pulse quadrupole-echo pulse sequence[4] was used in order to obtain more uniform excitation over the wide spectral width:

$$135°_x - 90°_{-x} - 45°_x - \tau - 135°_y - 90°_{-y} - 45°_y\ \tau - \text{acquire}$$

The phase of the second half of the sequence was cycled periodically by 180°. A τ delay of 20 μs was used, short enough to minimize distortions and intensity loss due to T_2 relaxation but long enough to reduce (but not completely eliminate) the effects of probe dead time. We note that this sequence refocuses quadrupolar interactions but not paramagnetic dipolar interactions. Despite possible paramagnetic dipolar interactions between the polyaniline and the inorganic framework, the absence of a refocusing pulse, for the τ interval used, did not produce significant phase or intensity distortions. Recycle delays sufficient to allow spin−lattice relaxation were used (typically 1 s, and checked with 10 s delay); a spectrum obtained with a long recycle delay of 100 s did not show any difference, indicating the absence of components with long relaxation times. Phasing was carried out on the time domain echo signal to place all of the signal in one channel; the echo maximum was then found by left-shifting an appropriate number of points to form a "free induction decay" (fid), which was multiplied by a 2 kHz exponential apodization function and Fourier transformed to yield a properly phased spectrum. A spectral width of 2 MHz with 16K data points was used. No notable sample orientation effects were observed.

Charge-Transport Measurements. Direct-current electrical conductivity and thermopower measurements were made on compactions of powder in pellet form and free-standing films. Conductivity measurements were performed in the usual four-probe geometry with 60 and 25 μm gold wires used for the current and voltage electrodes, respectively. Measurements of the pellet cross-sectional area and voltage probe separation were made with a calibrated binocular microscope. Conductivity data were obtained with a computer-automated system described elsewhere.[5] Thermoelectric power measurements were made by using a slow ac technique with 60 μm gold wires serving to support and conduct heat to the sample, as well as to measure the voltage across the sample resulting from the applied temperature gradient. In both measurements, the gold electrodes were held in place on the sample with a conductive gold paste.

Syntheses. *Preparation of $V_2O_5{\cdot}nH_2O$ Xerogel.* A HVO_3 solution was obtained by dissolving 4.0 g (32.8 mmol) of $NaVO_3$ in 250 mL of distilled H_2O, and passing the solution through a H^+ ion-exchange column, packed with 30 g of Dowex-50 × 2−100 resin. Upon standing, the yellow HVO_3(aq) polymerizes within 24−96 h to a V_2O_5 sol which thickens to become a V_2O_5 gel. The gel was then poured on glass substrates, and the excess water was allowed to evaporate upon standing in air. The dark red film formed on the surface of glass has the chemical formula $V_2O_5{\cdot}nH_2O$ ($n \sim 1.6$ depending on ambient humidity). The dry film can be peeled off to a free-standing film or it can be ground to a powder for subsequent use.

Synthesis of Bulk Polyaniline. An amount of 103 g (452 mmol) of $(NH_4)_2S_2O_8$ was dissolved in 150 mL of water and then added to a solution containing 20.0 g (215 mmol) of aniline with 300 mL of 1 M HCl(aq). The mixture was stirred in air at 0 °C for 1 h and then at room temperature for 3 h. The black precipitate was isolated by filtration, washed with water then acetone, and dried in air. The product was identified by its characteristic infrared spectrum.[6]

Preparation of $(PANI)_{0.44}V_2O_5{\cdot}1.15H_2O$ Film. In a typical reaction, 2.0 g (21.5 mmol) of aniline was mixed with 30 mL of distilled H_2O (the mixture is not necessarily a homogeneous solution). To this was added 0.5 g (2.37 mmol) of V_2O_5 xerogel film. The mixture was allowed to stand at room temperature for 24 h in air. The black pieces of film were isolated by filtration, washed with acetone, and dried in vacuum. Elemental anal. calcd for $(C_6H_4NH)_{0.44}V_2O_5{\cdot}1.15H_2O$: C, 13.04%; H, 1.85%; N, 2.53%; V, 42.00%. Found: C, 12.92%; H, 1.53%; N, 2.53%; V, 41.69%.

Preparation of $(PANI)_{0.19}V_2O_5{\cdot}0.6H_2O$ Film. An amount of 0.1 g (1.1 mmol) of aniline was dissolved in 20 mL of distilled H_2O, followed by addition of 0.6 g (2.84 mmol) of V_2O_5 xerogel film. The mixture was allowed to stand at room temperature for 5 h in air. The product was isolated by filtration, washed with acetone, and dried in vacuum. Elemental anal. calcd for $(C_6H_4NH)_{0.19}V_2O_5{\cdot}0.6H_2O$: C, 6.50%; H, 1.02%; N, 1.26%; V, 48.46%. Found: C, 6.37%; H, 1.16%; N, 1.33%; V, 47.08%.

Preparation of $(PANI)_{0.77}V_2O_5{\cdot}0.26H_2O$ Powder. An amount of 0.5 g (2.38 mmol) of V_2O_5 xerogel (fine powder) was added in 85 mL of 3.5 wt % of aniline aqueous solution. The mixture was stirred at room temperature for 16 h in air. The black powder was isolated by filtration, washed with acetone, and dried in vacuum. Anal. Calcd for $(C_6H_4NH)_{0.77}V_2O_5{\cdot}0.26H_2O$: C, 21.59%; H, 1.70%; N, 4.20%; V, 39.73%. Found: C, 21.59%; H, 2.02%; N, 4.07%; V, 39.51%. By changing the aniline/V_2O_5 ratio and solvent amount, different stoichiometric products can be obtained. The interlayer spacings of all samples calculated from the X-ray powder diffraction patterns are equal to 13.94 ± 0.02 Å.

Preparation of (poly-2,6-dimethylaniline)$_{0.4}V_2O_5{\cdot}0.5H_2O$. An amount of 0.1 g (0.83 mmol) of 2,6-dimethylaniline was mixed with 50 mL of H_2O, followed by addition of 0.35 g (1.66 mmol) of film of V_2O_5 xerogel. The mixture was allowed to stand at room temperature without stirring for 14 h in air. The black film was isolated by filtration, washed with acetone, and dried in air. Elemental anal. calcd for $(C_8H_8NH)_{0.4}V_2O_5{\cdot}0.5H_2O$: C, 16.13%; H, 1.91%; N: 2.35%; V, 42.85%. Found: C, 15.13%; H, 2.40%; N, 2.36%; V, 40.68%. The interlayer spacing calculated from X-ray diffraction is 14.57 ± 0.02 Å.

Extraction of Polyaniline from $(PANI)_xV_2O_5{\cdot}nH_2O$. Basic Solution. An amount of 0.15−0.25 g of $(PANI)_xV_2O_5{\cdot}nH_2O$ was mixed with 100 mL of 2 wt % NaOH(aq) and stirred at room temperature for 17 h. The black residue was isolated by filtration, washed copiously with H_2O and 1.0 M HCl(aq) followed by acetone, and dried in vacuum. The product was identified to be the emeraldine salt of polyaniline by infrared spectroscopy.

Acidic Solution. $(PANI)_xV_2O_5{\cdot}nH_2O$ was mixed with excess 2 M HCl(aq) and stirred at room temperature for 2 days. The black residue was isolated by filtration, washed with H_2O and then acetone, and dried in vacuum. It was identified to be the emeraldine salt of polyaniline.

Preparation of $(C_6H_5NH_3)_{0.4}V_2O_5{\cdot}0.4H_2O$. Under a nitrogen atmosphere, 0.5 g (2.37 mmol) of powdered $V_2O_5{\cdot}1.8H_2O$ reacted with 2.1 g (9.48 mmol) of anilinium iodide in 50 mL of methylene chloride at room temperature. After stirring for 2 days, the dark-blue product was isolated by filtration and washed with acetone. The composition of the product obtained from thermogravimetric analysis (TGA) under oxygen flow was $(C_6H_5NH_3)_{0.4}V_2O_5{\cdot}0.4H_2O$.

(4) Siminovitch, D. J.; Raleigh, D. P.; Olejniczak, E. T.; Griffin, R. G. *J. Chem. Phys.* ***1986***, *84*, 2556.

(5) (a) Diel, B. N.; Inabe, T.; Lyding, J. W.; Schock, K. F., Jr.; Kannewurf, C. R.; Marks, T. J. *J. Am. Chem. Soc.* **1983**, *105*, 1551−1567. (b) Lyding, J. W.; Marcy, H. O.; Marks, T. J.; Kannewurf, C. R. *IEEE. Trans. Instrum. Meas.* **1988**, *37*, 76−80.

(6) (a) Kim, Y. H.; Foster, C.; Chiang, J.; Heeger, A. J. *Synth. Met.* **1988**, *26*, 49−59. (b) Ohira, M.; Sakai, T.; Takeuchi, M.; Kobayashi, Y.; Tsuji, M. *Synth. Met.* **1987**, *18*, 347−352. (c) Wudl, F.; Augus, R. O., Jr.; Lu, F. L.; Allemand, P. H.; Vachon, D. J.; Nowak, M.; Liu, Z. X.; Heeger, A. J. *J. Am. Chem. Soc.* **1987,** *109*, 3677−3684. (d) Vachon, D.; Angus, R. O.; Lu, F. L.; Nowak, M.; Liu, Z. X.; Schaffer, H.; Wudl, F.; Heeger, A. J. *Synth. Met.* **1987,** *18*, 297−302. (e) Lu, F.-L.; Wudl, F.; Nowak, M.; Heeger, A. J. *J. Am Chem. Soc.* **1986**, *108*, 8311−8313.

Results and Discussion

The objective of this study was 3-fold: (a) to characterize in detail the redox intercalation reaction of aniline with V_2O_5 xerogel and the subsequent polymerization chemistry associated with this system, (b) to intercalate anilinium ions in V_2O_5 xerogel without polymerization and induce their intralamellar polymerization in a subsequent step, and (c) to better understand the effects of oxygen on the structure, composition, physicochemical properties, and electrical behavior of PANI/V_2O_5 nanocomposites. We begin with a discussion of the synthetic chemistry and polymer characterization, followed by infrared, NMR spectroscopic, magnetic, and charge-transport studies of the products. We then address the issue of electron accounting and the role of molecular oxygen in the intercalative polymerization of aniline.

Reaction of Aniline with V_2O_5 Xerogel and Product Characterization. The intercalation of aniline in V_2O_5 xerogel is a redox reaction in which aniline is oxidatively polymerized and V_2O_5 is reduced. It occurs instantly upon contact of the xerogel with aniline (aqueous solution) and is associated with an immediate and dramatic color change to dark blue. Despite this, the reaction takes several hours to go to completion because of the diminishing diffusion of the growing guest species into the inner layers of the host. Generally, if the solvent containing the aniline is able to swell the xerogel, the intercalation reaction is fast. In fact, V_2O_5 xerogel did not intercalate neat aniline presumably because it is not readily swelled by it. When organic solvents which swell the xerogel, such as DMSO, DMF, etc., were used, we found significant amount of co-intercalated solvent and a smaller polymer fraction. Thus far, water seems to be the most suitable solvent for this redox intercalation because a lot of it is expelled from the slightly hydrophobic intragallery space, allowing more polymer to be inserted. The films obtained from the reaction showed good lamellar order, but the compositional homogeneity of the product was difficult to control. In other words, the polymer/V_2O_5 ratio throught the sample may not be constant. Reducing the particle size of the xerogel increases the reaction rate and avoids the homogeneity problem but, at the same time, decreases the lamellar order of the products, as judged by the XRD pattern. When a wet xerogel (preswollen) of V_2O_5 was used, the reaction was complete within minutes but the final product was nearly amorphous, and sometimes the V_2O_5 framework was severely disrupted as judged by the dramatic changes in the V−O stretching region of the infrared spectrum. Acetonitrile does not swell the V_2O_5 xerogel at room temperature, and we observed no reaction between V_2O_5 film and aniline in this solvent at room temperature. Nevertheless, when a fine powder of V_2O_5 was used or the reaction was carried out at reflux temperature, intercalation did occur, but the products were relatively poorly crystalline.

The FTIR spectrum of $(PANI)_xV_2O_5{\cdot}nH_2O$ shows the characteristic IR pattern of emeraldine salt in the region 1000−1600 cm^{-1} (Figure 1). The three strong peaks below 1000 cm^{-1} are characteristic of the V_2O_5 framework. The intercalated polyaniline can be extracted by digesting the V_2O_5 matrix with 2 M HCl(aq) or 2% NaOH(aq) and characterized by infrared spectroscopy to be very similar to bulk polyaniline (Figure 1).

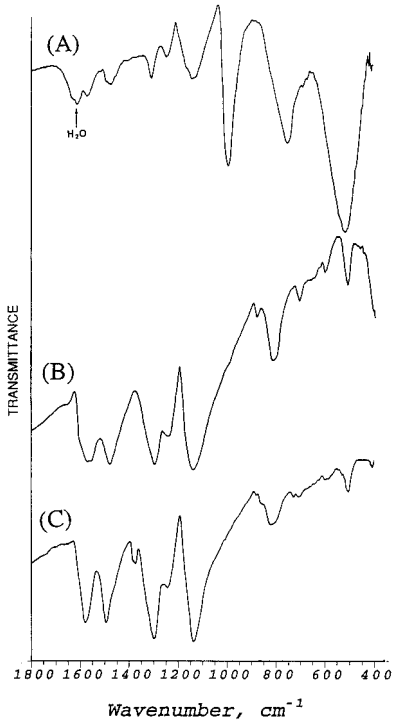

Figure 1. FT-IR spectra (KBr pellets) of (A) $(PANI)_xV_2O_5{\cdot}nH_2O$, (B) bulk polyaniline (emeraldine salt), and (C) polyaniline extracted from $(PANI)_xV_2O_5{\cdot}nH_2O$.

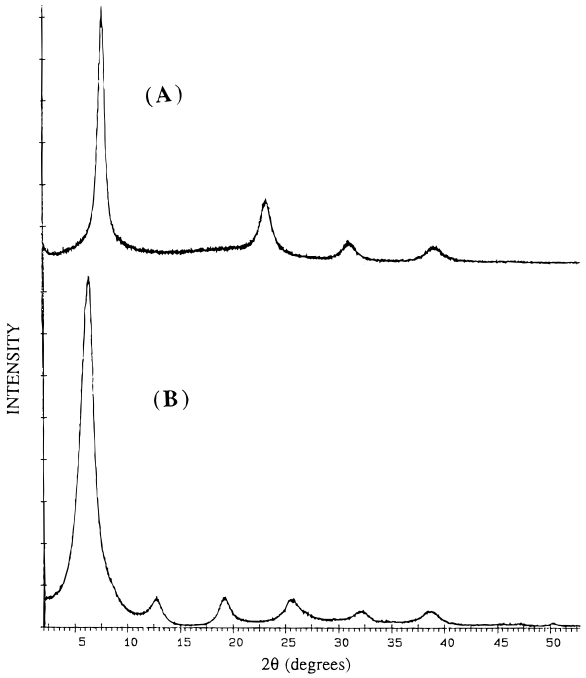

Figure 2. Reflection-mode X-ray diffraction patterns of films of (A) V_2O_5 xerogel and (B) $(PANI)_{0.44}V_2O_5{\cdot}1.15H_2O$.

Upon intercalation, the interlayer spacing of V_2O_5 xerogel expands from 11.55 to 13.94 Å. Only (00*l*) reflections are observed in the X-ray diffraction pattern which is a typical pattern for quasi-crystalline layered materials see Figure 2. The 2.39 Å interlayer expansion is the result of removing one layer of H_2O (approximately 2.8 Å) and inserting a PANI monolayer. Therefore, the net expansion due to an intercalated monolayer of polyaniline corresponds to 5.2 Å and is comparable to that found in $(PANI)_xFeOCl$ in which parallel polymer chains lie ordered between the host sheets.[2] A similar

Scheme 1

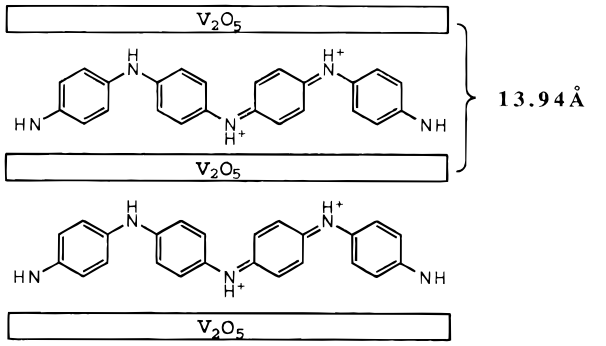

Scheme 2

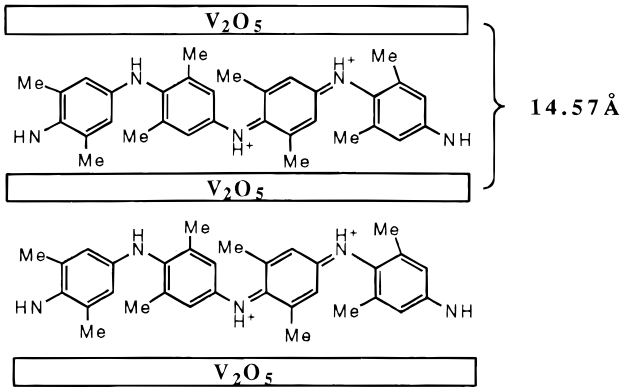

qualitative model can be proposed for $(PANI)_xV_2O_5{\cdot}nH_2O$, where the 2-fold symmetry axis bisecting the C−N−C angle, is perpendicular to the V_2O_5 slabs (see Scheme 1).

This model is further supported by the fact that insertion of poly(2,6-dimethylaniline) in V_2O_5 gives a material with slightly larger interlayer spacing of 14.57 Å. This is due to the spatial requirements of the two methyl groups in the 2,6 position of the benzene rings whose planes do not lie parallel to the metal oxide slabs (Scheme 2). Along the stacking direction, the X-ray scattering coherence lengths (calculated from the Scherrer formula[7]) of the V_2O_5 xerogel and $(PANI)_xV_2O_5nH_2O$ are similar and range between ∼110 and 120 Å .

The X-ray diffraction patterns of $(PANI)_xV_2O_5{\cdot}nH_2O$ and V_2O_5 with the X-ray beam perpendicular to the layers are shown in Figure 3. This diffraction geometry allows us to examine the structural integrity and intralayer atomic organization of the V_2O_5 slabs. The two diffraction patterns are nearly identical proving that the intralayer framework of V_2O_5 is structurally preserved after inserting polyaniline, consistent with a truly topotactic reaction. This is in accord with the IR spectral data in the range 380−1000 cm^{-1}, which show little change before and after intercalation, and with the TEM electron diffraction studies of $(PANI)_xV_2O_5{\cdot}nH_2O$ and $V_2O_5{\cdot}nH_2O$ which show very similar Bragg ring patterns. The *d* spacings calculated from the observed Bragg rings are in good agreement with the *d* spacings obtained by transmission-mode X-ray diffraction.

Electron microscopic examination shows the surfaces of $(PANI)_xV_2O_5{\cdot}nH_2O$ films to be continuous and relatively homogeneous with a clearly lamellar morphology. The TEM image of V_2O_5 xerogel and $(PANI)_xV_2O_5{\cdot}nH_2O$ studied in our laboratory did not always show the fiber nature as seen by Livage and co-workers.[8] Very often the image obtained could be interpreted as folded sheets.

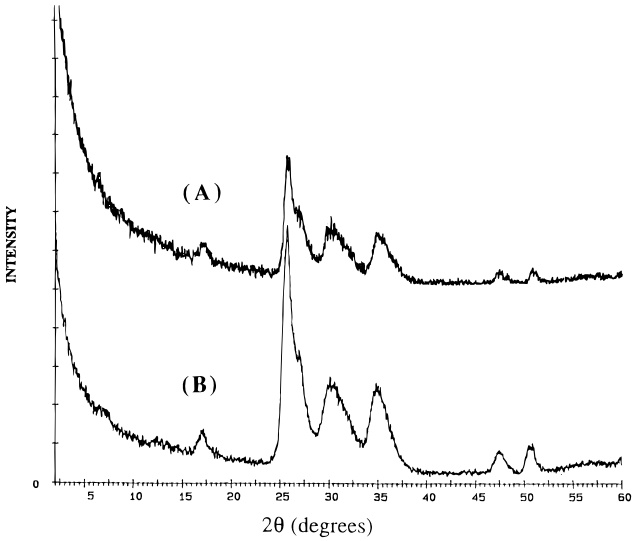

Figure 3. Transmission-mode X-ray diffraction patterns of films of (A) V_2O_5 xerogel and (B) $(PANI)_{0.44}V_2O_5{\cdot}1.15H_2O$. (In this experiment, the incident X-ray beam was perpendicular to the film. The detector is moving along the 2θ angle while the sample along the θ angle.)

Reactions with high aniline/V_2O_5 molar ratio tend to result in products containing a small fraction of co-inserted anilinium molecules. The anilinium ions cannot be removed by washing with acetone or pumping under vacuum at room temperature; however, they disappear upon aging (i.e., by remaining in air for several weeks or months). This phenomenon was also observed in $(PANI)_xFeOCl$.[2] There is no weight loss during aging, suggesting that the anilinium ions were either polymerized or oxidatively coupled to other polymer chains rather than evaporated from the sample. The anilinium molecules can be removed by heating the sample at 185 °C under low pressure for several days as judged by the lower carbon content of the heated samples. Interestingly, when the heating was performed in an evacuated sealed tube for 3 days, the polyaniline IR peaks did not change but the intensity of the peak at around 740 cm^{-1}, which is due to the V−O vibration of V_2O_5 host, decreased dramatically indicative of an increased number of V^{4+} centers. This suggests that electron transfer occurred from the guest polymer to the V_2O_5 framework.

Role of Ambient Oxygen. In the beginning stages of this work we carried out the intercalative polymerization reactions under inert atmosphere. Further observations, however, suggested that the products obtained from reactions carried out under air displayed different properties. For example, under air, we observed that the reaction completion times were shorter and the products tended to possess better lamellar order. Further indications about the divergence of the two types of products came from the magnetic properties, which showed a higher spin number in the nitrogen-prepared samples, and from the electrical properties,

(7) Scherrer formula: $D = (0.9\lambda)/\beta \cos\theta$. *D*: average crystallite size normal to the reflection plane in Å. λ: radiation wavelength (Å). β: half-width in radiants. θ = Bragg angle in degrees.

(8) Livage, J.; Gharbi, N.; Leroy, N. C.; Michaud, M. *Mater. Res. Bull.* **1978**, *13*, 1117−1124.

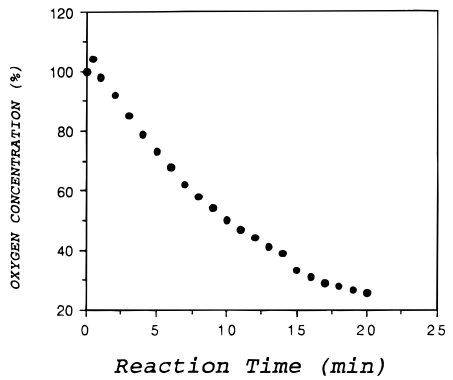

Figure 4. Oxygen concentration versus reaction time during the intercalation of aniline (aqueous solution saturated with oxygen) in V_2O_5 xerogel. (The 100% level indicates saturation and the aniline to V_2O_5 ratio in this reaction was one).

which showed that the samples prepared in air were more conductive. These facts are related to the aforementioned interesting observation that co-inserted anilinium ions, trapped in the gallery space, polymerize in air. Since samples prepared in air had higher conductivities and better lamellar order, we concentrated our efforts on those. The samples prepared under nitrogen are essentially different compounds and must be studied separately.[9]

The reaction steps of aniline and V_2O_5 in air are very complicated. Several reactions, both concomitant and sequential, may be involved: (a) the oxidative polymerization of aniline, (b) the recombination of H^+ with V_2O_5, (c) the acid−base interaction of H^+ and aniline, (d) the reduction of V_2O_5, (e) the reaction between V_2O_5 and O_2, (f) the insertion of aniline/anilinium in the host lattice, and (g) the reaction between aniline oligomers and O_2. An overall intercalative polymerization reaction is given in eq 1.

$$x\mathrm{C_6H_5NH_2} + \mathrm{V_2O_5}\cdot n\mathrm{H_2O} + (2x - 3y)/2\mathrm{O_2} \rightarrow (\mathrm{C_6H_4NH})_{x-y}(\mathrm{C_6H_5NH_3})_y\mathrm{V_2O_5}\cdot m\mathrm{H_2O} + (2x - 3y)/2\mathrm{H_2O_2} + (n - m)\mathrm{H_2O} \quad (1)$$

When the polyaniline/anilinium ratio equals 0.5 ($2x = 3y$), no oxygen is needed since all protons released from the aniline radical cation react with another aniline molecule to form anilinium ions. The polyaniline/anilinium ratio was estimated by isolating the polymer from the V_2O_5 matrix and comparing this to the total organic content of the material. For freshly prepared samples, we found the polymer to be greater than 75% of the total organic component.

Oxygen participation in the reaction was proven by using an oxygen monitor. The solvent was saturated with oxygen and its concentration was monitored as the aniline/V_2O_5 reaction proceeded (Figure 4). The decreasing oxygen concentration, during the reaction indicates that oxygen is consumed. In a control experiment, V_2O_5 xerogel was reacted with alkali-metal iodide, such as KI, which inserts K^+ ions to give $K_xV_2O_5\cdot n\mathrm{H_2O}$. No oxygen was consumed during the entire reaction period (30 min), which suggests the consumption of oxygen is associated with the formation of polymer. In another such experiment, the reaction was run with $(NH_4)_2S_2O_8$ as the oxidant instead of the V_2O_5 xerogel.

(9) Kanatzidis, M. G.; et al., work in progress.

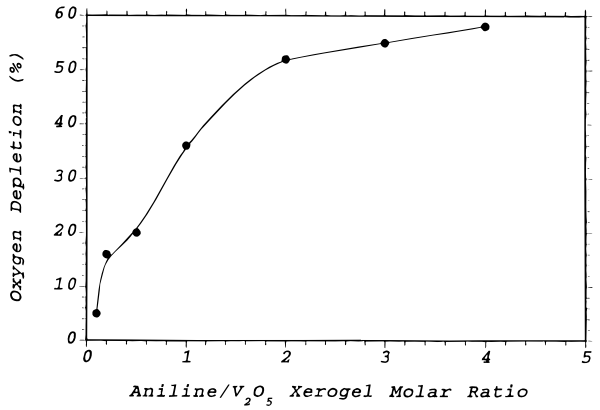

Figure 5. Oxygen consumption versus aniline/V_2O_5 ratio. (At 0% consumption, the aqueous solution is saturated with oxygen.) Data taken at $t = 15$ min.

Scheme 3. Head-to-Tail Oxidative Coupling of Aniline Oligomers

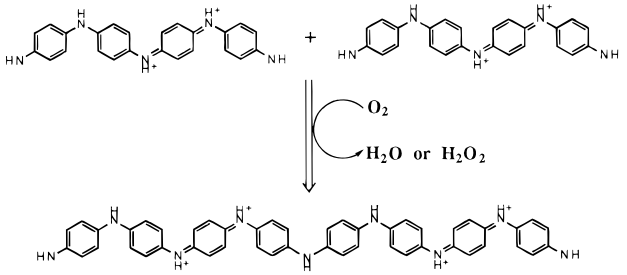

Only a very little oxygen consumption was observed, amounting to less than 4% of that observed for the xerogel at comparable reaction times. This result confirms unequivocally the importance of vanadium in oxygen reduction. The oxygen consumption also depends on the aniline/V_2O_5 molar ratio, where high aniline/V_2O_5 ratios consumed more oxygen (see Figure 5). The oxygen consumption saturates at very high ratios, suggesting that the aniline-to-oxygen electron transfer is a diffusion-limited process. When the oxygen is depleted from the solution and not replenished, the reaction, and particularly the polymerization, slows down significantly, giving rise to products with a higher fraction of anilinium ions in the gallery.

Oxygen not only is involved in the intercalative polymerization reaction but also changes the properties of the resulting products. Aging the samples in the presence of O_2, causes two separate reactions to occur: first, the reduced V_2O_5 framework is partially reoxidized, and second, polyaniline chains inside the V_2O_5 gallery couple oxidatively to form longer chains (see Scheme 3). Since the aged samples are chemically distinct from those obtained fresh after isolation, from now on they will be called π-$(PANI)_xV_2O_5\cdot n\mathrm{H_2O}$ in order to distinguish them from the freshly made ones, which we will simply refer to as $(PANI)_xV_2O_5\cdot n\mathrm{H_2O}$.

The polyaniline extracted from π-$(PANI)_xV_2O_5\cdot n\mathrm{H_2O}$ is less soluble in organic solvents such as THF, DMF, and acetone than polyaniline extracted from the fresh samples, suggesting that the former has a higher molecular weight. The anilinium peaks in the IR spectra are not visible in the π-samples which, as mentioned above, have the same organic content their precursors. Furthermore, the thermal stability, magnetic susceptibility, and charge-transport properties also

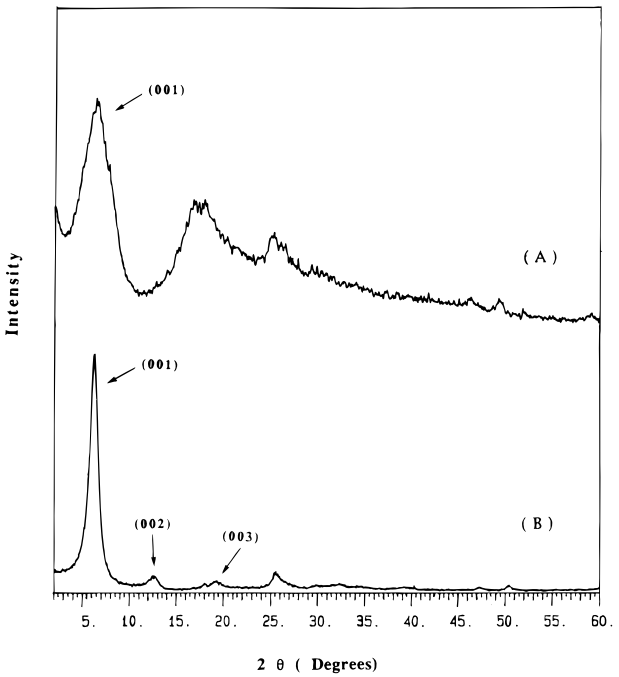

Figure 6. Reflection-mode X-ray diffraction patterns of films of (A) $(C_6H_5NH_3)_{0.4}V_2O_5{\cdot}0.4H_2O$ and (B) π'-$(PANI)_{0.4}V_2O_5{\cdot}0.4H_2O$.

change significantly upon aging (vide infra). More direct evidence that the PANI chains are longer in the π-samples comes from the GPC results (vide infra).

Intercalation of Anilinium and Postintercalative Polymerization. The detection of anilinium ions in the products and their intralamellar, postintercalative polymerization upon standing in air, suggested that we may be able to prepare an all-anilinium intercalate which may undergo a similar polymerization reaction, in the solid state, upon standing. To avoid anilinium ion oxidation by the V_2O_5 xerogel, we chose to use the iodide salt. Indeed, in the absence of oxygen anilinium intercalates in vanadium oxide gels according to eq 2.

$$x C_6H_5NH_3^+ I^- + V_2O_5{\cdot}nH_2O \rightarrow (C_6H_5NH_3)_xV_2O_5{\cdot}mH_2O + (x/2)I_2 \quad (2)$$

The intercalation is confirmed by the net increase of ca. 5.1 Å in the interlayer distance (see Figure 6). The very broad (00*l*) diffraction peak corresponds to a very short coherence length, perpendicular to the layers, which is estimated to be ~30 Å according to the Scherrer equation. This is considerably smaller than the ~120 Å found in the V_2O_5 xerogel itself indicating considerable disruption of the lamellar stacking order. The presence of anilinium is unambiguously established by infrared spectroscopy. Exposure to air induces profound changes in the infrared spectrum of the material where the anilinium vibrations gradually disappear and the strong characteristic pattern of the emeraldine salt form of polyaniline becomes dominant. The conversion to PANI is complete in 3−4 weeks, as judged from infrared spectroscopy. The material resulting from this process will be referred to here as π'-$(PANI)_{0.4}V_2O_5{\cdot}0.4H_2O$ to distinguish it from the related aged materials described above. The (00*l*) peak in the X-ray diffraction pattern, shown in Figure 6B, of π'-$(PANI)_{0.4}V_2O_5{\cdot}0.4H_2O$ narrows dramatically compared to that of its precursor indicating that the polymerization is intralamellar, forming a

Scheme 4

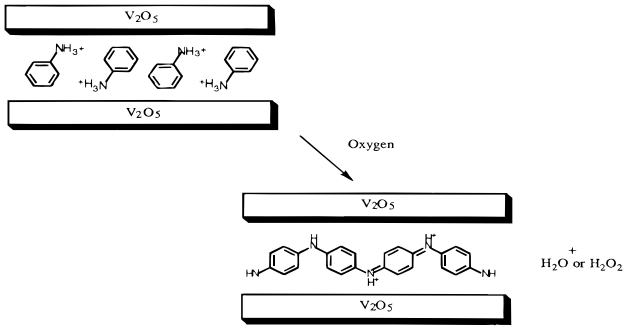

monolayer of polyaniline chains inside the framework. The estimated coherence length along the layers stacking axis increases 3-fold to ~90 Å, suggesting a significantly improved lattice organization. The overall reaction is shown in Scheme 4.

The changes in position and shape of the vibration peaks of the vanadium oxide framework are also significant. The V=O vibration peak shifts from 990 to 1000 cm^{-1}, while the V−O−V vibration peaks shift from 852 and 530 cm^{-1} to 750 and 496 cm^{-1}, respectively. These changes are due to the greater number of V^{4+} centers in $(C_6H_5NH_3)_{0.4}V_2O_5{\cdot}0.4H_2O$ than in π'-$(PANI)_{0.4}$-$V_2O_5{\cdot}0.4H_2O$, which is confirmed by the magnetic susceptibility measurements presented below. After digestion of the V_2O_5 framework, the absorptions of the extracted PANI from π'-$(PANI)_{0.4}V_2O_5{\cdot}0.4H_2O$ occur at slightly higher energies than bulk PANI, which suggests that the polymer has lower molecular weight; see GPC results below.

The mechanism of this remarkable all-solid-state intralamellar polymerization must be intimately coupled to the ability of vanadium centers[10] to activate oxygen, which is the primary and ultimate electron acceptor in this process. Simple anilinium salts are not oxidized to polyaniline under the experimental conditions employed here. Therefore, vanadium oxide plays a direct role in this redox event, and this is consistent with its ability to catalyze several oxidation reactions of organic molecules.[10] That oxygen removes electrons from the metal oxide framework can be seen by the decrease of the magnetic susceptibility of the material following this intralamellar polymerization.

Gel Permeation Chromatography and Molecular Weight Analysis. Estimates of the molecular weight of the various polymer samples extracted from the intercalation compounds were obtained with gel permeation chromatography (GPC) analysis. A 0.5% LiCl solution of NMP was used as an eluent at room temperature. Although the GPC technique has been applied to analyze the molecular weight of polyaniline,[11] unfortunately previous studies among different groups have not been carried under identical experimental conditions, and a general consensus on its molecular

(10) (a) Genti, G.; Pinelli D.; Trifiro, F. *J. Mol. Catal.* **1990**, *59*, 221−231. (b) Ross, R. A.; Fairbridge, C. *Can. J. Chem.* **1984**, *62*, 1483−1491.

(11) (a) Genies, E,. M.; Syed, A. A.; Tsintavis, C. *Mol. Cryst. Liq. Cryst.* **1985**, *121*, 181−185. (b) Watanabe, A.; Mori, K.; Iwasaki, Y.; Nakamura, J. *J. Chem. Soc., Chem. Commun.* **1987**, 3−4. (c) Wei, Y.; Hsuech, K.; Tang, X.; Sun, Y. *Polym. Prepr.* **1989**, *30*, 226−227. (d) MacDiarmid, A. G.; Epstein, A. J. In *European Physical Society Industrial Workshop, Science and Applications of Conducting Polymers;* IOP Publishing: Lofthus, Norway, 1990.

Table 1. Molecular Weights of Bulk and Extracted Poly(aniline)[a]

material	M_p	M_n	M_w	polydispersity
bulk PANI	32 000	7 700	69 000	8.9
PANI from $(PANI)_xV_2O_5{\cdot}nH_2O$	19 000	14 000	30 000	2.1
PANI from π-$(PANI)_xV_2O_5{\cdot}nH_2O$	27 000	17 700	44 500	2.5
PANI from π'-$(PANI)_xV_2O_5{\cdot}nH_2O$	14 000	12 300	19 800	1.6

[a] M_n (number-average molecular weight) $= (\sum_i N_i M_i)/(\sum_i N_i)$. M_w (weight-average molecular weight) $= (\sum_i N_i M_i^2)/(\sum_i N_i M_i)$. M_p: molecular weight at the maximal absorption position. The molecular weight reported here are self-consistent, but the absolute values may not be correct because the polystyrene standards used for calibration may not be good models for the solution behavior of polyanilines.

weight (MW) has not yet been reached. Therefore, for comparison purposes in this work we also examined by GPC bulk PANI.[12]

The polymer extracted from all samples as well as bulk PANI were converted to the emeraldine base by treating with 1% NaOH(aq). The THF-extractable portion for all samples has very low molecular weight (<600). The molecular weight of the NMP-soluble portion gave monomodal peak distributions corresponding to high MW see Table 1. The molecular weight of extracted PANI is strikingly lower than that of the bulk polymer, reflecting the structurally restricted polymerization conditions in the intragallery space of the xerogel. Notice, however, the superior polydispersity (M_w/M_n ratio) achieved by the intralamellar polymerization. This is perhaps a unique feature of the intercalative polymerization reaction and most likely carries mechanistic implications. It underscores the potential of this reaction in achieving polymers with controlled MW. We found that polyanilines extracted from various $(PANI)_xV_2O_5{\cdot}nH_2O$ products had slightly different MW distributions. This is because the exact extend of polymerization cannot be strictly controlled. The highest average molecular weight (M_w) measured for polyaniline extracted from $(PANI)_xV_2O_5{\cdot}nH_2O$ was ~30 000 with a considerable portion of the sample (~15−20%) at molecular weight around 1300. On the other hand, polyaniline extracted from π-$(PANI)_xV_2O_5{\cdot}nH_2O$ had molecular weights up to ~44 500 with no appreciable small MW fraction. This strongly suggests that, in air, the polyaniline chains continue to grow, long after the intercalation reaction is over.

NMP solutions of the polymer extracted from π'-$(PANI)_xV_2O_5{\cdot}nH_2O$ gave GPC traces with a broad monomodal molecular mass distribution with a peak maximum corresponding to a M_w of ~19 800. The overall smaller molecular weight for this polymer, relative to that found in $(PANI)_xV_2O_5{\cdot}nH_2O$ and π-$(PANI)_xV_2O_5{\cdot}nH_2O$, is rationalized by the fact that polymerization in the π'-phase relies on the solid-state diffusion of anilinium and its oligomers with no solvent or exchange with similar species from a surrounding solution. Furthermore, the limited amount of anilinium ions in the precursor material and the absence of excess anilinium ions coming from the solution to couple with intercalated oligomers limits polymer growth, much more so than in the $(PANI)_xV_2O_5{\cdot}nH_2O$ systems formed in situ.

Thermogravimetric Analysis. The thermal stability of these materials in nitrogen and in air was examined by TGA experiments. All samples show a small moisture loss at temperatures starting at below 100 °C. This is followed by a continuous weight loss up to 700 °C for the freshly prepared and 600 °C for the aged π-phases. The weight loss between 100 and 700 °C is due to the oxidative decomposition of the polymer and the loss of trace amounts of water from V_2O_5. Since the degree of polymerization varies somewhat from sample to sample, as suggested by GPC analysis, the weight loss patterns in the TGA diagrams vary slightly as well. The thermal stability of $(PANI)_xV_2O_5{\cdot}nH_2O$ is better than that of its aged counterpart under either nitrogen or oxygen flow. At first, this might seem counterintuitive, given the higher average MW in the aged samples. As will be shown below, the aging process results in fewer V^{4+} centers (and more V^{5+} centers) rendering the framework more oxidizing, which degrades the polymer chains more easily. As expected, the thermal stability of all phases is better when the TGA experiment is carried out under nitrogen flow than under oxygen flow. The thermal stability of π-PANI under nitrogen flow is higher than that extracted from the fresh samples, consistent with its higher average MW.

Under nitrogen flow both samples, $(C_6H_5NH_3)_{0.4}V_2O_5{\cdot}0.4H_2O$ and π'-$(PANI)_xV_2O_5{\cdot}nH_2O$, lose weight continuously from ~100 to 900 °C due to oxidative degradation of anilinium and PANI by the vanadium oxide framework. Interestingly, $(C_6H_5NH_3)_{0.4}V_2O_5{\cdot}0.4H_2O$ shows slightly better thermal stability even though π'-$(PANI)_xV_2O_5{\cdot}nH_2O$ contains polymer. Again we attribute this to the higher relative amounts of V^{5+} in the latter material.

^{2}H NMR Spectroscopic Studies. Detailed information about temperature-dependent motional dynamics, specifically "flipping" of deuterated aromatic rings and chain motion, can be obtained using wide-line ^{2}H quadrupolar-echo NMR spectra. Such studies were published previously for bulk PANI and variations in the fraction of rings undergoing flips were observed with temperature and sample type.[13] In this study we used ^{2}H quadrupolar-echo NMR to investigate deuterated PANI intercalated in the vanadium oxide xerogel. In diamagnetic solids deuterium NMR spectra are generally interpreted in terms of a nuclear quadrupole coupling constant (NQCC) and its corresponding asymmetry parameter η. These two parameters, while characteristic of the chemical type (bonding environment) of the deuterium atom, are also affected by molecular motions that result in motional averaging. The deuterium chemical shift anisotropy is generally negligible. The result is a spectrum that is symmetric

(12) It should be noted that the MW values reported here should be used only on a relative basis since they probably do not represent the true MW of the polymers. The reason for the discrepancy lies in the assumption that polystyrene in NMP is a good model polymer for polyaniline in NMP.

(13) (a) Kaplan, S.; Conwell, E. M.; Richter, A. F.; MacDiarmid, A. G. *Macromolecules* ***1989***, *22*, 1669. (b) Kaplan, S.; Conwell, E. M.; Richter, A. F.; MacDiarmid, A. G. *J. Am. Chem. Soc.* ***1988***, *110*, 7647. (c) Devreux, F.; Bidan, G.; Syed, A. A.; Tsintavis, C. *J. Phys.* ***1985***, *46*, 1595.

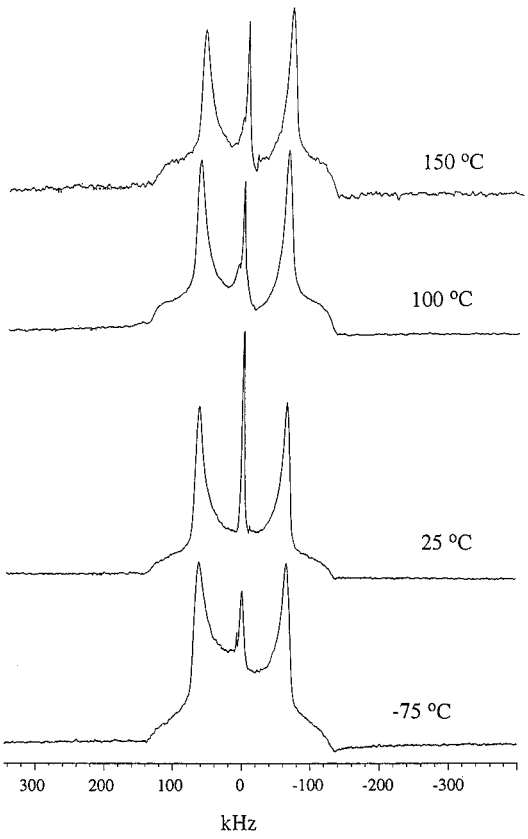

Figure 7. Quadrupolar echo ^{2}H NMR spectra of $(PANI)_{0.44}V_2O_5{\cdot}0.71H_2O$ as a function of temperature. All spectra were recorded with repetition delay of 1 s.

about its center frequency, even in the presence of partial orientation effects.

Deuterium quadrupolar-echo spectra of perdeuterated bulk PANI were obtained as a function of temperature. Unlike the temperature-dependent spectra observed in the PANI/FeOCl system[2] the spectral parameters of perdeuterated $(PANI)_{0.44}V_2O_5{\cdot}nH_2O$ are essentially constant between −75 and 150 °C, (see Figure 7). The sharp central peak presumably arises from water molecules undergoing isotropic reorientation. The deuterium atoms attached to the nitrogen atoms of PANI could not be observed. We were also unable to obtain any spectra of specifically deuterated PANI(N,N-d_2)−$V_2O_5{\cdot}nH_2O$ sample with the normal pulse interval of $\tau = 20\ \mu$s. This could be due to a short T_2 relaxation time, possibly due to motions of the amino deuteron and/or paramagnetic effects; it is interesting that the correspondingly labeled bulk emeraldine salt of PANI also yielded a very weak signal. Another possibility is that the signal is inhomogeneously broadened by paramagnetic centers (either on the host or in the polymer chain). We note that these NH groups could be interacting, via hydrogen bonding, with vanadyl, or V−O−V groups in the framework and thus be experiencing paramagnetic influence.

The spectra from in this temperature region exhibit a characteristic sharp deuterium powder pattern (Pake doublet) with the splitting between the two most intense features being 129 kHz. From these data we conclude that the polymer chains in these materials are not undergoing ring flips up to 150 °C, contrary to what was observed previously, for bulk PANI[13] and for PANI−FeOCl,[2] where motion of the aromatic rings is taking place at elevated temperatures. The static behavior of aromatic rings of the intercalated PANI confirms the serious spatial confinement experienced by the polymer in the intralamellar space of $V_2O_5{\cdot}nH_2O$. This confinement is probably reinforced by hydrogen bonding between the metal oxide framework and the NH groups in the polymer.

Electron Paramagnetic Resonance (EPR) Spectroscopy. EPR spectroscopy is an excellent probe to study the nature of free spins in $(PANI)_xV_2O_5{\cdot}nH_2O$, since both the emeraldine form and the reduced V_2O_5 framework are paramagnetic and EPR active. The EPR spectrum of $(PANI)_xV_2O_5{\cdot}nH_2O$ features an intense, broad signal at $g = 1.975$ with ΔH_{pp} in the range 75−100 G. At lower temperatures, the EPR signal intensity of $(PANI)_xV_2O_5{\cdot}nH_2O$ is slightly enhanced but does not change in shape and width. This signal originates from the reduced V_2O_5 framework, and it is qualitatively similar to that observed in the $A_xV_2O_5{\cdot}nH_2O$ (A = Na, K, Cs) family.[14] The original hyperfine splitting, arising from the ^{51}V ($I = {}^7/_2$) nucleus,[3e] disappears after intercalation due to dipolar exchange broadening. Interestingly, the typical strong and sharp EPR resonance arising from the massive polarons of bulk polyaniline was not observed.[15] This confirms that the polaron spins on polyaniline are in very close proximity (<10 Å) to the paramagnetic V^{4+} centers and participate in significant magnetic exchange interactions. The characteristic EPR signal of emeraldine is observed only after removal of the V_2O_5 matrix. This is additional independent evidence that in $(PANI)_xV_2O_5{\cdot}nH_2O$ the mixing of polyaniline and V_2O_5 is at the molecular level and not simply an intimate physical mixture, consistent with the structural model of Scheme 1. The same phenomenon has also been observed in polyaniline intercalated in zeolite,[16] in $Ni(CN)_2NH_3$,[17] and in FeOCl.[2]

The aged, π-phase, shows a similar but less intense EPR signal (the g value and ΔH_{pp} do not change), suggesting fewer free spins on V_2O_5 due to partial reoxidation of the host. Nevertheless, the reoxidation of V_2O_5 has not reached preintercalation levels since the hyperfine pattern from the ^{51}V ($I = {}^7/_2$) nucleus is not observed in the EPR spectrum even after 2 years.

The room-temperature EPR spectra of $(C_6H_5NH_3)_{0.4}V_2O_5{\cdot}0.4H_2O$ and π'-$(PANI)_{0.4}V_2O_5{\cdot}0.4H_2O$ also show broad symmetric signals centered at $g \sim 1.96$ with peak width (ΔH_{pp}) is 660 and 130 G, respectively. The larger ΔH_{pp} in the former (increased magnetic exchange broadening) is consistent with larger V^{4+} concentration in this compound compared to π'-$(PANI)_{0.4}V_2O_5{\cdot}0.4H_2O$ and is in agreement with the magnetic susceptibility data for these materials. The sharp EPR resonance arising from the polarons in PANI is not observed in this sample either, consistent with significant magnetic

(14) Liu, Y. J.; Cowen, J. A.; Kaplan, T. A.; DeGroot, D. C.; Schindler, J. L.; Kannewurf, C. R.; Kanatzidis, M. G., *Chem. Mater.* **1995**, *7*, 1616−1624.

(15) (a) Ioffe, N. T.; Kogen, Y. L.; Mairanovskii, V. G. *Synth. Met.* **1990**, *37*, 74−75. (b) Lapkosk, M.; Genies, E. M. *J. Electroanal. Chem.* **1990**, *279*, 158−168. (c) Javadi, H. H. S.; Laversanne, R.; Epstein, A. J.; Kohli, R. K.; Scherr, E. M.; MacDiarmid, A. G. *Synth. Met.* **1989**, *29*, E439−444.

(16) (a) Enzel, P.; Bein, T. *J. Phys. Chem.* **1989**, *93*, 6270−6272. (b) Bein, T.; Enzel, P. *Synth. Met.* **1989**, *29*, E163-E168. (c) Enzel, P.; Bein, T. *J. Chem. Soc., Chem. Commun.* **1989**, 1326−1327.

(17) Wu, C. G.; Marcy, H. O.; DeGroot, D. C.; Schindler, J. L.; Kannewurf, C. R.; Kanatzidis, M. G. *Synth. Met.* **1991**, *41/43* 693−698.

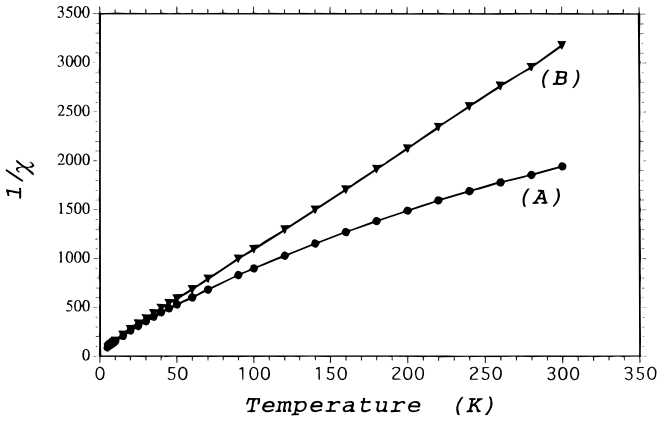

Figure 8. Temperature dependence of inverse magnetic susceptibility for $(PANI)_{0.24}V_2O_5{\cdot}nH_2O$ (A); χ is the total measured molar susceptibility; (B) molar susceptibility corrected for χ_{TIP}.

coupling interactions between the organic guest species and the paramagnetic inorganic framework.

Magnetic Susceptibility Studies. In accordance with the EPR data, variable-temperature magnetic susceptibility measurements for all $PANI/V_2O_5{\cdot}nH_2O$ samples show paramagnetic behavior. The paramagnetic contribution from polyaniline is relatively small,[18] and therefore the net magnetic moment comes mostly from V^{4+} species in V_2O_5. The magnetic susceptibility data can be separated into two components: a Curie–Weiss and a temperature-independent paramagnetic (TIP) component, see eq 3.

$$\chi_m = \chi_{Curie-Weiss} + \chi_{TIP} \qquad (3)$$

$$\chi_m = \frac{C}{T-\theta} \qquad \theta = \text{Weiss constant}$$

TIP is found in transition-metal ions where the interacting d levels have been split by the ligand field.[19] The TIP susceptibility is considerably smaller than the Curie–Weiss paramagnetism and is clearly noticeable in the high-temperature data. The magnitude of χ_{TIP} depends on the size of the energy gap between the ground and first excited state, ΔE.[19] A significant amount of TIP was detected in the $A_xV_2O_5{\cdot}nH_2O$ (A = K, Cs) class of xerogel bronzes[14] and was found to depend on the degree of reduction of V_2O_5, where the coordination of the metal is thought to be a distorted square-pyramidal geometry of approximate C_{2v} symmetry.[3] This gives rise to a very small energy gap ΔE, which allows the χ_{TIP} to be observed in these materials.

Figure 8 shows a typical plot of the variation of $1/\chi_m$ as a function of temperature of $(PANI)_{0.24}V_2O_5{\cdot}nH_2O$. The Weiss constant is always very small (less than a few degrees), and in this case is −1.35 K. The room-temperature magnetic moments, μ_{eff}, of $(PANI)_xV_2O_5{\cdot}nH_2O$ with various x values are shown in Table 2.

Table 2. Room-Temperature Magnetic Moment and Temperature-Independent Paramagnetism of $(PANI)_xV_2O_5{\cdot}nH_2O$ versus x

x	total μ_{eff} (μ_B)	Curie–Weiss[a] μ_{eff} (μ_B)	$104\chi_m$ (TIP)
0.21	0.97	0.88	0.75
0.24	1.21	0.98	2.0
0.25	1.17	0.87	2.5
0.29	1.02	0.90	1.0
0.44	0.87	0.61	1.6
0.48	1.25	0.78	4.0
0.72	0.92	0.75	1.2
$(C_6H_5NH_3)_{0.4}V_2O_5{\cdot}0.4H_2O$	1.30	0.80	3.4
π'-$(PANI)_{0.4}V_2O_5{\cdot}0.4H_2O$	0.87	0.62	0.65

[a] Corrected for TIP van Vleck paramagnetism.

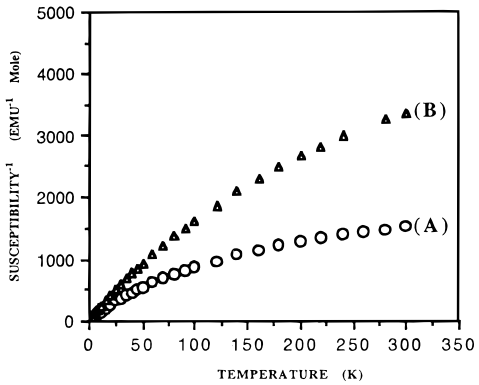

Figure 9. Temperature dependence of inverse magnetic susceptibility of (A) $(PANI)_{0.48}V_2O_5{\cdot}0.33H_2O$ and (B) π-$(PANI)_{0.48}$-$V_2O_5{\cdot}0.33H_2O$. The curvature in the data is due to the substantial temperature independent paramagnetism (see ref 14).

Two observations become immediately obvious from this table. First, there is no direct relationship between the polymer content and magnetic moment. Second, the total μ_{eff} is always smaller than the theoretically expected value assuming all the electrons released from aniline during oxidative polymerization, were transferred to V_2O_5. The lower μ_{eff} values are consistent with our findings presented above that a significant fraction of the electrons released from aniline (or anilinium) are transferred to oxygen and not to V_2O_5. The complicated interactions between oxygen, polyaniline, and reduced V_2O_5 makes it is difficult to quantitate the degree of reduction of V_2O_5 in all $(PANI)_xV_2O_5{\cdot}nH_2O$ simply using μ_{eff} values.[20]

Upon aging, the samples show a decreased magnetic susceptibility consistent with reoxidation of some V^{4+} centers to V^{5+} (see Figure 9). The reoxidation process is slow and levels off with time. The χ_{TIP} of $(PANI)_{0.48}$-$V_2O_5{\cdot}nH_2O$ also decreases upon aging and is in agreement with results reported on the $A_xV_2O_5{\cdot}nH_2O$ family.[14]

That the V_2O_5 framework acts as an electron relay between the reducing guest and oxygen is further supported by the magnetic susceptibility data of $(C_6H_5$-$NH_3)_{0.4}V_2O_5{\cdot}0.4H_2O$ and π'-$(PANI)_{0.4}V_2O_5{\cdot}0.4H_2O$, where the latter shows smaller magnetic susceptibility than

(18) (a) Ginder, J. M.; Richter, A. F.; MacDiarmid, A. G.; Epstein, A. J. *Solid State Commun.* **1987**, *63*, 97–101. (b) Fite, C.; Cao, Y.; Heeger, A. J. *Solid State Commun.* **1989**, *70*, 245–247. (c) Wudl, F.; Angus, R. O.; Lu, F. L.; Allemand, P. M.; Vachon, D. J.; Nowak, M.; Liu, Z. X.; Heeger, A. J. *J. Am. Chem. Soc.* **1987**, *109*, 3677–3684.

(19) (a) Earnshaw, A. *Introduction to Magnetochemistry*; Academic Press: New York, 1968. (b) Boudreaux, E. A.; Mulay, L. N. *Theory and Applications of Molecular Paramagnetism*; John Wiley and Sons: New York, 1976 pp 122–124. (c) Gladney, H. M.; Swalen, J. D. *J. Chem. Phys.* **1965**, *42*, 1999–2009. (d) Drago, R. S. *Physical Methods in Chemistry;* W. B. Sanders Co.: Philadelphia, 1977 pp 417–426.

(20) We have attempted to quantitate the degree of reduction of V_2O_5 host by X-ray photoelectron spectroscopy (XPS). The V^{5+} peak of $(PANI)_xV_2O_5{\cdot}nH_2O$ has a broad shoulder which is not observed in the V_2O_5 xerogel. This shoulder is due to the overlapping of V^{5+} and V^{4+} peaks. However, the change of the binding energy, the peak shape of V^{4+}, and the significant overlap between the V^{5+} and V^{4+} peaks, pose serious difficulties in determining a reliable V^{4+}/V^{5+} ratio.

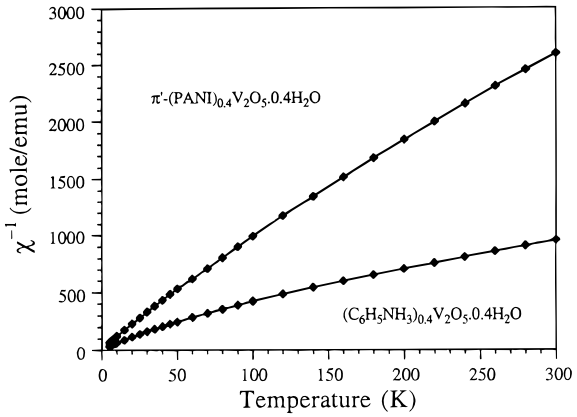

Figure 10. Temperature dependence of inverse magnetic susceptibility of $(C_6H_5NH_3)_{0.4}V_2O_5{\cdot}0.4H_2O$ and π'-$(PANI)_{0.4}$-$V_2O_5{\cdot}0.4H_2O$.

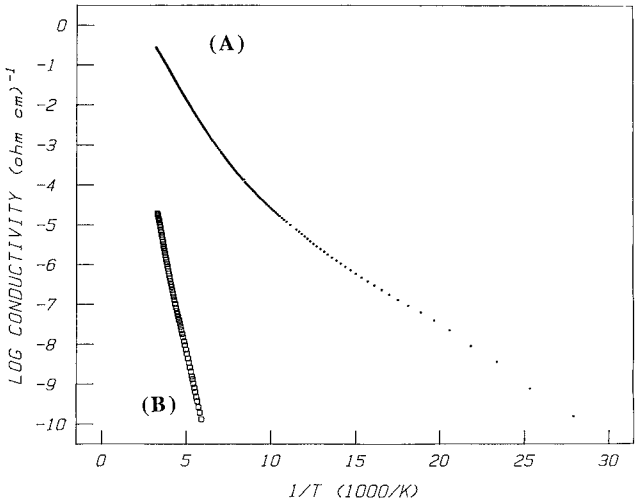

Figure 11. Four-probe variable-temperature electrical conductivity data of films of (A) $(PANI)_{0.44}V_2O_5{\cdot}0.56H_2O$ and (B) Pristine V_2O_5 xerogel.

its anilinium precursor, indicating fewer unpaired electrons. Both compounds are paramagnetic exhibiting Curie−Weiss behavior with a contribution of temperature-independent van Vleck paramagnetism (TIP, see Figure 10).

Charge Transport Properties. *Electrical Conductivity.* The insertion of polyaniline in $V_2O_5{\cdot}nH_2O$ generates a hybrid system in which two different types of low-dimensional electrical conductors coexist at the molecular level in a dimensionally constrained environment. There are two types of charge carriers in these materials, small polarons (electrons) associated with the d^1 (V^{4+}) centers found on the vanadium oxide lattice, and massive polarons located on the polyaniline backbone.[21] Charge transport in these nanocomposite materials would depend on the relative mobilities of these two different kind of carriers.

The electrical conductivity of $(PANI)_xV_2O_5{\cdot}nH_2O$ is 10^4 times higher than pristine V_2O_5 (see Figure 11). In all samples, the conductivity which is almost exclusively electronic under our experimental conditions, increases with rising temperature as has been observed in most

(21) (a) Javadi, H. H.; Cromack, K. R.; MacDiarmid, A. G.; Epstein, A. J. *Phys. Rev. B* **1989**, *39*, 3579−3584. (b) Javadi, H. H. S.; Laversanne, R.; Epstein, A. J.; Kohli, R. K.; Scherr, E. M.; MacDiarmid, A. G. *Synth. Met.* **1989**, *29*, E439−444. (c) Zuo, F.; Angelopoulos, M.; MacDiarmid, A. G.; Epstein, A. J. *Phys. Rev. B* **1989**, *39*, 3570−3578.

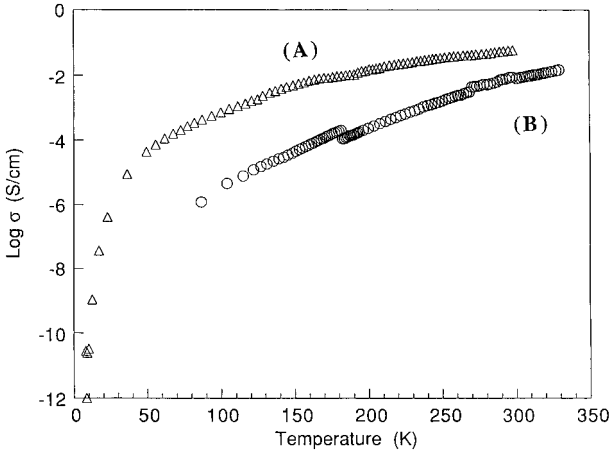

Figure 12. Four-probe variable-temperature electrical conductivity data of films of $(PANI)_{0.30}V_2O_5{\cdot}0.56H_2O$ prepared in (A) air and (B) N_2 atmosphere.

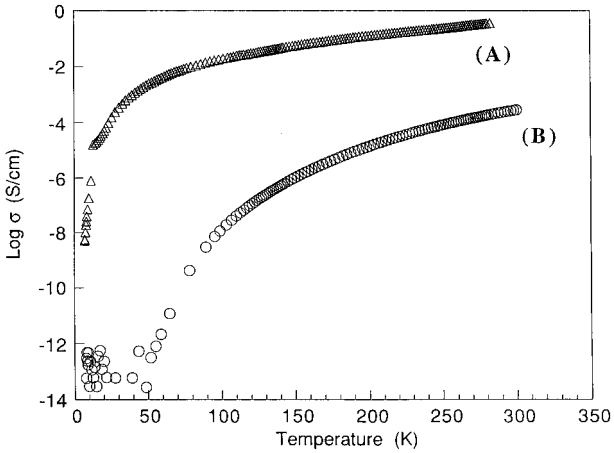

Figure 13. Four-probe variable-temperature electrical conductivity data of (A) $(PANI)_{0.48}V_2O_5{\cdot}nH_2O$ (film) and (B) $(PANI)_{0.48}V_2O_5{\cdot}nH_2O$ (pressed pellet). *n* varies between 0.5 and 1.3.

intercalated compounds and conjugated polymers.[1,2] For a similar polyaniline/V_2O_5 ratio, the material prepared in air has higher conductivity than that prepared under nitrogen (see Figure 12). The room-temperature conductivity of the PANI/$V_2O_5{\cdot}nH_2O$ samples can vary from 10^{-4} to 10^0 S/cm, depending on age, polymer content and MW, and sample morphology. Since age, polymer content, and MW are all independent parameters in these materials, this leads to no direct relationship between the conductivity and polyaniline/V_2O_5 ratios. The age factor directly affects the conjugation and chain length of polyaniline inside the V_2O_5 host, while the PANI content determines the interchain and chain-to-host interactions. The highest conductivities will be expected in samples in which both the polymer content and polymer chain length is high. The films are considerably anisotropic with conductivity parallel to the layers being at least 100 times higher than perpendicular to them.

There is a strong dependence of the electrical conductivity on sample morphology. Generally, the conductivities of film samples are 100−1000 times higher than those of pressed pellets because of better interparticle continuity. Figure 13 shows a typical variable temperature conductivity of $(PANI)_xV_2O_5{\cdot}nH_2O$ in film and pressed pellet forms.

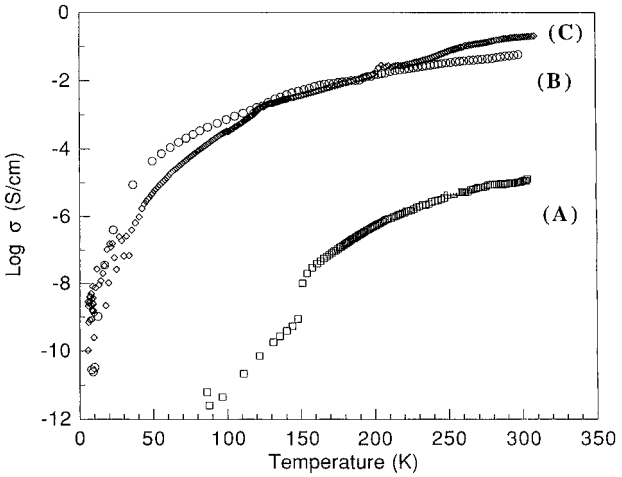

Figure 14. Four-probe variable-temperature electrical conductivity data of pressed pellets of $(PANI)_{0.48}V_2O_5 \cdot 0.33H_2O$: (A) freshly prepared, (B) aging for 16 months, and (C) aging for 31 months.

Upon aging for several months the conductivity of $(PANI)_xV_2O_5 \cdot nH_2O$ increased slowly and then leveled off to a certain value (see Figure 14). Over the period of 1.5 years up to 4 orders of magnitude increase has been observed, without significant changes in the XRD patterns of these materials. Since the number of carriers in the V_2O_5 layers decreases upon aging, charge transport through them is expected to decrease. The increased conductivity with aging, therefore, must come from the formation of longer chains of polyaniline via oxidative coupling after exposure to air. Apparently, the oxidative coupling of polyaniline continues until the polymer chains become too long to be able to diffuse. This limits the further growth of the polymer chains and explains the leveling off of the magnitude of the electrical conductivity.

The electrical conductivity of π'-$(PANI)_xV_2O_5 \cdot nH_2O$ is 3 orders of magnitude higher than that of its precursor $(C_6H_5NH_3)_{0.4}V_2O_5 \cdot 0.4H_2O$, consistent with the presence of PANI. However, the conductivity of the π'-phase is still approximately an order of magnitude lower than that of π-$(PANI)_xV_2O_5 \cdot nH_2O$. This is attributed to the smaller polymer chain length in the former.

As expected, the polyaniline extracted from π- and π'-$(PANI)_xV_2O_5 \cdot nH_2O$ is more conductive by an order of magnitude than that extracted from $(PANI)_xV_2O_5 \cdot nH_2O$ (e.g., 1 vs 0.1 S/cm).

Thermoelectric Power. The electrical properties discussed above are strongly influenced by the effects of sample morphology, particle size, and interparticle boundaries. Thermoelectric power (TP) is less affected by interparticle contact resistance. It can provide valuable information as to the true nature of charge transport within the material such as the intrinsic (electronic band structure) or extrinsic (particle contacts) nature of the thermally activated behavior. The room-temperature thermoelectric power of powder samples does not show a definitive trend based on polymer content, in agreement with the fact that neither the degree of reduction of the V_2O_5 framework nor the molecular weight are directly related to the polymer/V_2O_5 ratio. Typical variable-temperature TP data of $(PANI)_xV_2O_5 \cdot nH_2O$ in pressed pellet and film forms are shown in Figure 15. The TP (i.e., Seebeck coefficient), of pressed pellets is large, negative with a weak temperature dependence from room temperature down to 220 K. Below 220 K, accurate measurements could not be made due to high sample resistance. The data unequivocally show that the freshly prepared materials are n-type semiconductors similar in behavior to the reduced xerogels $A_xV_2O_5 \cdot nH_2O$, which show an x-dependent TP with a weak temperature variation.[14] The $(PANI)_xV_2O_5 \cdot nH_2O$ samples, however, typically display smaller TP than $A_xV_2O_5 \cdot nH_2O$ when comparing samples with similar degrees of framework reduction. This implies that the PANI chains play a role in the charge-transport properties of the nanocomposites. The extent of this role depends on the sample age, i.e., polymer MW. For further comparison, the TP of bulk (emeraldine salt) polyaniline is different from that of the $(PANI)_xV_2O_5 \cdot nH_2O$ samples. It shows metallic behavior and its TP can have a negative or positive sign depending on the degree of protonation.[22] Therefore, the charge-transport properties of $(PANI)_xV_2O_5 \cdot nH_2O$ are dominated by the small polarons of the reduced V_2O_5 framework but not to the extent found in $A_xV_2O_5 \cdot nH_2O$. This is consistent with the formation of short polymer chains which inhibit facile chain-to-chain charge transport and suggests that the mobility of the small polarons in the inorganic slabs is significantly higher than the mobility of the carriers in polyaniline. The charge transport appears more favorable through V_2O_5 layers, although assistance from the polymer chains, particularly in the direction perpendicular to the layers seems appreciable.

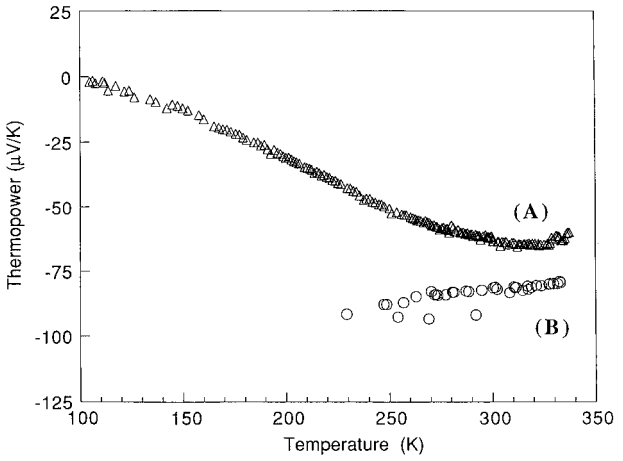

Figure 15. Variable-temperature thermoelectric power data of (A) $(PANI)_{0.44}V_2O_5 \cdot 1.3H_2O$ (film) and (B) $(PANI)_{0.44}V_2O_5 \cdot 0.33H_2O$ (pressed pellet).

That the TP of the film samples is generally smaller than that of the pressed powder samples (see Figure 15) could be explained by the fact that in the films, which are morphologically smooth and continuous, some V_2O_5 slabs are probably long enough to span several conducting particles. At the same time some PANI chains could act as bridges between such particles by intercalating two different sets of V_2O_5 stacks. This gives rise to longer carrier mean free paths, lower activation barriers for carrier transport, and a better electrical communication between the particles, illustrated in Figure 16. In contrast, when the films are ground to a powder the average length of a V_2O_5 slab

(22) (a) Park, Y. W.; Lee, Y. S.; Park, C. *Solid State Commun.* **1987**, *63*, 1063. (b) Zuo, F.; Angelopoulos, M.; MacDiarmid, A. G.; Epstein, A. *J. Phys. Rev.* **1987**, *B36*, 3475−3478.

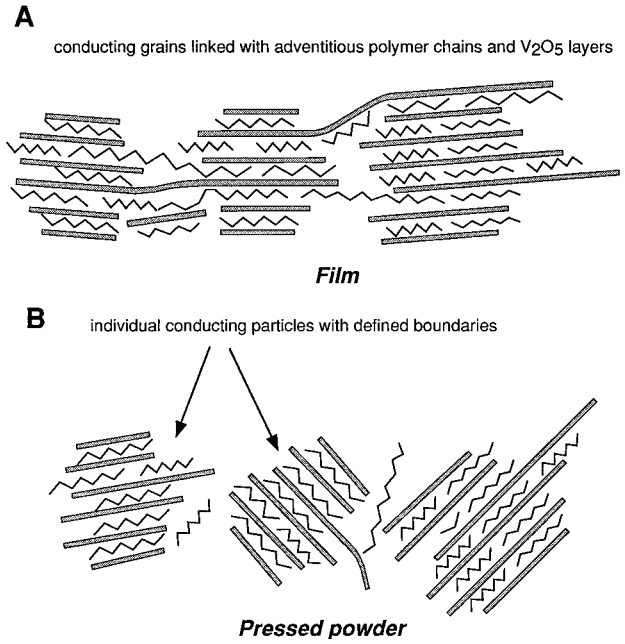

Figure 16. Schematic illustration of the nanoscale level structural differences of samples with different morphology, in this case films, as prepared by in situ intercalative polymerization (A) and pressed ground powders of same (B).

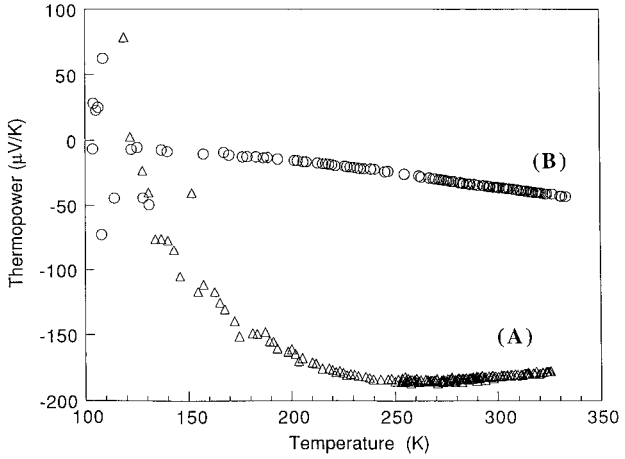

Figure 17. Variable-temperature thermoelectric power data of pressed pellets of (A) $(PANI)_{0.44}V_2O_5 \cdot nH_2O$ and (B) π-$(PANI)_{0.44}V_2O_5 \cdot nH_2O$.

could be reduced and the increased interparticle boundaries thus generated would frustrate such electrical communication pathways, forcing the charge transport to rely more on tunneling through insulating interparticle boundaries. Therefore, the polyaniline inside the V_2O_5 is probably playing a more important role in the charge-transport properties of the film samples than it does in the ground powder samples.

The TP values of samples of π-$(PANI)_xV_2O_5 \cdot nH_2O$ are also negative but smaller than those of their precursors. The smaller magnitude and temperature dependence suggest a n-type *metallike* behavior (see Figure 17). The considerably more facile charge transport exhibited by the aged samples is explained by the postintercalative polymer growth in the gallery space, as was demonstrated by the various physicochemical studies presented above. Longer polymer chains increase the carrier mean free path and reduce the frequency of carrier hopping from chain to chain raising the mobility of the polarons in polyaniline and facilitating charge transport through the intercalated polymer. Therefore, polyaniline plays an enhanced role in the charge-transport properties of the aged samples. However, the influence of V_2O_5 in the charge transport of the aged samples is still crucial.

Concluding Remarks

The redox reaction between aniline and V_2O_5 xerogel produces electrically conductive, anisotropic, lamellar polymer nanocomposites in varying PANI/V_2O_5 ratios and good one-dimensional order. These materials feature alternating layers of vanadium oxide and polymer. All spectroscopic and physicochemical evidence shows that the emeraldine salt form of PANI is formed. The experimental data presented here suggest that the polymerization proceeds concomitantly with intercalation, but chain growth, which is critical to the development of the intercalated polymer, occurs primarily inside the xerogel. The polymer chains appear fixed in the intralamellar space, and the ring flips observed in the bulk form of polyaniline are frozen in these materials. Therefore, there is considerable bonding interaction between the organic and the inorganic components probably due to NH- - -O−V hydrogen bonding. The chain growth events are intimately tied with electron transfer to molecular oxygen in which the V_2O_5 xerogel acts as a catalyst. The recognition that molecular oxygen is directly involved in these intercalative polymerization reactions is an important milestone in our understanding of how these nanocomposites form. It will help us in the future to better exploit this synthetic methodology and generalize it to prepare other novel materials of the type reported here and elsewhere.[23,24]

Aging in air causes the partial oxidation of the inorganic framework of $(PANI)_xV_2O_5 \cdot nH_2O$ and oxidative coupling of the polyaniline inside the interlamellar space, which results in the formation of longer polymer chains with higher electrical conductivity. The charge-transport properties of the fresh samples are dominated by transport in the reduced V_2O_5 host, whereas in the aged samples the polymer plays a more significant role.

Acknowledgment. Financial support from the National Science Foundation (DMR-93-06385) is gratefully acknowledged. M.G.K. is a Camille and Henry Dreyfus Teacher Scholar, 1993−1995. At NU this work made use of Central Facilities supported by NSF through the Materials Research Center (DMR-91-20521). The NMR data were obtained on instrumentation housed in the Max T. Rogers NMR Facility at Michigan State University. This work made use of the SEM facilities of the Center for Electron Optics at Michigan State University. We thank professor James Yesinowski for help with the NMR spectra and for fruitful discussions.

CM9600236

(23) Liu, J.-Y.; Kanatzidis M. G. *Inorg. Chem.* **1993**, *32*, 2989−2991.
(24) Liu, J.-Y.; Kanatzidis M. G. *Chem. Mater.* **1995**, *7*, 1525−1533.